

Basic Science: Original Paper

Optimization of processing parameters for the analysis and detection of embolic signals

Nizamettin Aydin *, Hugh S. Markus

Division of Clinical Neuroscience, St George's Hospital Medical School, Cranmer Terrace, London SW 17 0RE, UK

Received 23 March 2000; received in revised form 19 June 2000; accepted 24 June 2000

Abstract

The fast Fourier transform (FFT), which is employed by all commercially available ultrasonic systems, provides a time-frequency representation of Doppler ultrasonic signals obtained from blood flow. The FFT assumes that the signal is stationary within the analysis window. However, the presence of short duration embolic signals invalidates this assumption. For optimal detection of embolic signals if FFT is used for signal processing, it is important that the FFT parameters such as window size, window type, and required overlap ratio should be optimized. The effect of varying window type, window size and window overlap ratio were investigated for both simulated embolic signals, and recorded from patients with carotid artery stenosis. An optimal compromise is the use of a Hamming or Hanning window with a FFT size of 64 (8.9 ms) or 128 (17.9 ms). A high overlap ratio should also be employed in order not to miss embolic events occurring at the edges of analysis windows. The degree of overlap required will depend on the FFT size. The minimum overlap should be 65% for a 64-point window and 80% for a 128-point window. © 2000 Elsevier Science Ltd. All rights reserved.

Keywords: Fast Fourier transform; Cerebral embolism; Ultrasonic; Doppler velocity measurement

1. Introduction

Asymptomatic cerebral emboli can be detected by transcranial Doppler ultrasound (Spencer et al., 1990). An embolus passing through the Doppler sample volume causes an increase in the power of the returned ultrasonic Doppler signal,

resulting in a short duration transient signal, which has maximum intensity across a narrow frequency range (Ringelstein et al., 1998). This technique has been shown to be highly sensitive and specific in animal models and in vitro (Markus and Tegeler, 1995), and embolic signals have been detected in patients with a wide variety of potential embolic sources. Detecting emboli with transcranial Doppler ultrasound (TCD) has clinical application in monitoring during surgical and other therapeutic interventions and possibly

* Corresponding author. Tel.: +44-20-87252461; fax: +44-20-87252950.

E-mail address: n.aydin@sghms.ac.uk (N. Aydin).

also in the identification of patients at high risk of stroke (Markus and Harrison, 1995).

TCD is conventionally used for embolic signal detection both due to the clinical importance of cerebral emboli, and the ease of fixing the probe against the skull for the prolonged recording periods required. The TCD systems in common use were designed for determining flow velocity (Aaslid et al., 1982) rather than for embolic signal detection. This has resulted in problems using these systems for embolic signal detection (Markus, 1995). Commercial Doppler ultrasound systems use the fast Fourier transform (FFT). The result, presented as sonogram, forms a time-frequency representation of Doppler signals which is obtained by first segmenting the data into frames, multiplying by a tapered window and then taking the FFT of each frame. This process is also known as short time Fourier transform or windowed Fourier transform (WFT). The assumption is made that the Doppler signals obtained from the blood flow are stationary within the analysis window. However, the presence of short duration embolic signals invalidates this assumption. New analysis methods may be more suited to embolic signal detection (Fan and Evans, 1994; Aydin et al., 1999) but until these are further developed and widely accepted, processing of embolic signals will continue to be based on the FFT. In view of the potential difficulties in applying the FFT to processing such signals, it is important that signal processing parameters are optimized for embolic signals (Markus et al., 1997). There has been little work in this area and no systematic evaluation of the effect of different parameters. Important FFT parameters which may influence the embolic signal detection are effective window size, window type and overlap ratio. It has been demonstrated that inadequate degree of overlap employed by commercially available systems may result in embolic signals being missed on the spectral display (Markus, 1995). Therefore in this study, the effect of varying these three parameters on embolic signal to blood ratio, embolic signal onset, and embolic signal temporal and frequency resolution was evaluated.

When using FFT analysis to study the frequency spectrum of signals, there are two basic

problems. We can only sample the signal for a limited time (analysis window, or processing frame), and the FFT only calculates results for certain discrete frequency values. The Fourier transform makes an implicit assumption that the signal within the processing frame is repetitive. Most real signals will have discontinuities at the ends of the processing frame so that when the FFT assumes the signal repeats it also incorporates discontinuities that are not there. Discontinuities can be eliminated if the signal falls smoothly to zero at each end of the processing frame. Multiplying the signal with a suitable window function can ensure this. Many window functions have been proposed in literature (Harris, 1978; Kay, 1988).

In a FFT analysis, there is a well-known trade-off between frequency resolution and time resolution determined by the length of the analysis window (Cohen, 1989). Since the FFT analysis depends critically on the choice of the window size, its application requires a priori information concerning the time evolution of the signal properties in order to make an a priori choice of the window. Once a window is chosen the resolution in both time and frequency is fixed in the entire time-frequency plane. The best combination of time-frequency resolution is not immediately obvious. This depends on the signal being processed and the optimal time-frequency resolution trade-off may be determined empirically or analytically.

Shifting the analysis window by less than the window length results in an overlapped FFT of the frames. The data frames are processed sequentially by sliding the window less than the frame size at each processing stage. Consequently, overlapping FFT windows produces higher dimensional WFTs. Some of the information in an overlapped WFT is redundant, and some of it is novel. A degree of overlap is required for embolic signal detection, but it has been demonstrated that some commercially available TCD systems have inadequate overlap. This may result in an underestimation of embolic signal intensity, or even embolic signals not appearing on the spectral display at all (Markus, 1995). This is a problem for short duration low intensity embolic signals such as those found in atrial fibrillation and

carotid artery stenosis. The optimal overlap ratio is not well documented. On the other hand, a higher overlap ratio than required will result in redundant data and imposes a computational burden on the system.

2. Methods

The embolic signals used for this study were recorded using a commercially available transcranial Doppler system (EME Pioneer TC4040) with a 2 MHz transducer. The recordings were made from the ipsilateral middle cerebral artery of patients with symptomatic carotid stenosis, but not at the time of carotid endarterectomy. Recordings had been made onto digital audiotape. We were primarily interested in optimizing the embolus to blood ratio, and therefore detection, of low intensity embolic signals. These have been most difficult to detect in the past particularly by automated detection systems. Therefore we selected 50 consecutive low intensity embolic signals which nevertheless met the standard criteria. Signals were identified by two experienced observers from both the FFT spectral display and the audio signal using conventional criteria (Ringelstein et al., 1998). The quadrature audio Doppler signal was exported to a PC for signal analysis. The sampling frequency of these signals was 7150 Hz and the data length was 2048 point (286 ms). The data were prepared to include embolic signals in the first 143 ms part of the total recordings. The second 143 ms of the data were used to calculate average background Doppler ultrasound power. In addition to the patient embolic signals, simulated embolic signals were used to determine the required overlap ratio for detecting short duration embolic signals reliably when a non-rectangular window was used prior to the FFT. They were produced by first generating a complex quadrature sinusoidal signal multiplied by a Gaussian window at the required duration, and then adding the white noise to this signal.

The following parameters were estimated: embolic signal intensity to background intensity ratio (EBR), half width maximum of the embolic signal power increase in the time domain (HWMT) as

an estimate of temporal resolution, half width maximum in the frequency domain (HWMF) as an estimate of frequency resolution, and absolute time of embolic signal onset (ESO) as an estimate of the accuracy of temporal localization. The EBR is defined as following:

$$\text{EBR} = 10 \log \frac{A_{\text{peak}}}{B_{\text{avg}}} \quad (1)$$

where A_{peak} is the power at frequency with maximum power, and B_{avg} is the average power of the background intensity. This was calculated by time and frequency averaging of the time-frequency analysis results using the second half of the total data;

$$B_{\text{avg}} = \frac{1}{t_2 - t_1} \sum_{t=t_1}^{t_2} \frac{1}{N} \sum_{v=1}^N S(t,v) \quad (2)$$

where $S(t,v)$ is the two-dimensional time-frequency distribution of the Doppler signal and N is the number of frequency points.

For time resolution, the time-frequency distribution of the embolic signal was integrated over all frequencies resulting in the instantaneous power of the signal (Williams et al., 1997). The HWMT was defined as the distance between the two points of 50% maximum of the normalized instantaneous power. For the frequency resolution, the time-frequency distribution of the embolic signal was integrated over all time resulting in the energy spectrum of the signal. The HWMF was defined as the distance between the two points of 50% maximum of the normalized energy spectrum. This parameter indicates the amount of the frequency spread depending on the windowing parameter considered.

The ESO was defined as the time at which the power increase reached 20% of the normalized instantaneous power curve. The ESO indicates how the time localization properties of the FFT are influenced by the windowing parameter considered. These were compared with the ESO values estimated from the instantaneous envelope (Boashash, 1992) of the quadrature Doppler signals.

For investigation of the effect of window size, the windowed Fourier transform was evaluated at intervals of one sample. Prior to the FFT, a Hanning window was applied. The FFT size was fixed to 512 and the parameters were evaluated for six different window sizes (16, 32, 64, 128, 256 and 512) or (2.24, 4.48, 8.95, 17.9, 35.8 and 71.61 ms, respectively). Since the time-frequency resolution of a FFT is dictated by the effective window size, this results in an interpolated time-frequency representation of the signal windowed by the effective window length. The process is equivalent to the 512 point FFT of W point signal (zero padded to 512 prior to the FFT) with 511 points overlap.

For investigation of the effect of window type, the windowed Fourier transform was also evaluated for each sample point, but both the FFT size and the effective window size were fixed to 64 points. The results were obtained for six different window types (rectangular (Boxcar), Bartlett, Hanning, Hamming, Blackman and Gaussian). These windows and corresponding frequency responses are illustrated in Fig. 1.

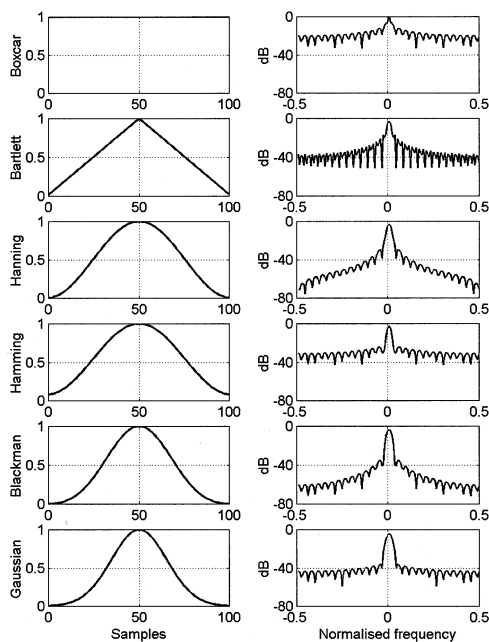


Fig. 1. Plots of some windowing functions and corresponding frequency responses.

In order to investigate the effect of overlap ratio on the detection of embolic signals two studies were performed. In the first, using the patient embolic signals, five overlap ratios (0, 25, 50, 75 and 98.4%) were studied with the FFT and effective window sizes fixed to 64 points. The second study concentrated on signals for which inadequate FFT overlap was likely to be a problem, i.e. short duration embolic signals, and used four simulated embolic signals having durations of 1.1, 2.2, 4.5 and 8.9 ms. Four FFT sizes (32, 64, 128 and 256) were considered to investigate the required overlap ratios. The evolution of the EBR, the ESO and the HWMT for four simulated signals were observed for all possible overlap ratios from 0 to 99% approximately. The Hanning window was used for all cases. Results were compared using paired t -tests. In view of the multiple comparisons made, a conservative P value of < 0.001 was considered as significant.

3. Results

3.1. Effect of window type

The results for six different window types are presented in Table 1A with the results of statistical comparisons in Table 2A. The highest EBR values were obtained for the Hamming (17.33 dB, SD = 2.43), Bartlett (17.33 dB, SD = 2.45), and Hanning windows (17.31 dB, SD = 2.40), and the lowest value for the boxcar window (17.03 dB, SD = 2.68) (see Table 2A). The best temporal resolution (HWMT) was obtained with the Gaussian window (9.85 ms, SD = 10.04). The mean frequency resolution (HWMF) was best for the rectangular window (246.05, SD = 212.40), though this window gave the worst temporal resolution (HWMT) (12.88, SD = 8.25). The ESO value for Gaussian window (64.26 ms, SD = 10.17, $P = 0.153$) was closest to the ESO value measured from time domain signal (64.59 ms, SD = 10.12). The boxcar window gave the worst mean ESO value (61.78 ms, SD = 10.53, $P < 0.0001$).

Table 1

Mean and standard deviations of the EBR, ESO, HWMT and HWMF for the 50 embolic signals^a

		EBR (dB) (SD)	ESO (ms) (SD)	HWMT (ms) (SD)	HWMF (Hz) (SD)
A ^a	Boxcar	17.03 (2.68)	61.78 (10.53)	12.88 (8.25)	246.05 (212.40)
	Bartlet	17.33 (2.45)	63.76 (10.16)	10.33 (9.60)	253.90 (199.00)
	Hanning	17.31 (2.40)	63.85 (10.18)	10.34 (9.72)	262.84 (202.73)
	Hamming	17.33 (2.43)	63.81 (10.17)	10.40 (9.70)	253.06 (199.54)
	Blackman	17.21 (2.29)	64.14 (10.18)	9.96 (9.85)	280.05 (204.64)
	Gaussian	17.14 (2.25)	64.26 (10.17)	9.85 (10.04)	291.50 (201.73)
B ^b	16	15.33 (2.30)	64.58 (10.12)	9.21 (9.76)	773.23 (157.77)
	32	16.32 (2.41)	64.50 (10.19)	9.55 (10.19)	485.04 (187.32)
	64	17.06 (2.76)	63.82 (10.21)	10.44 (9.73)	337.06 (195.36)
	128	17.12 (3.23)	62.19 (10.23)	12.35 (8.69)	275.17 (243.49)
	256	16.48 (3.45)	57.65 (10.69)	17.66 (7.22)	231.25 (210.72)
	512	15.51 (3.48)	43.36 (16.11)	30.83 (5.06)	225.72 (211.00)
C ^c	0%	16.10 (2.87)	62.70 (10.85)	7.15 (9.17)	213.03 (160.96)
	25%	16.68 (2.52)	63.24 (10.16)	7.24 (8.88)	232.06 (197.49)
	50%	17.01 (2.56)	62.65 (12.43)	8.06 (9.70)	253.29 (198.27)
	75%	17.20 (2.44)	63.69 (10.23)	8.77 (9.00)	261.99 (197.91)
	98.4%	17.31 (2.40)	63.85 (10.18)	10.34 (9.72)	262.84 (202.73)
Instantaneous envelope	–	64.59 (10.12)	–	–	–

^a FFT and window sizes were fixed to 64 and a 98.4% overlap ratio was employed.

^b FFT size was fixed to 512 and a Hanning window with 99.8% overlap ratio was employed.

^c FFT size was fixed to 64 and a Hanning window was employed.

3.2. Effect of window size

The results are presented in Tables 1B and 2B. The best time localization was obtained with a 16 point window size (64.58 ms, SD = 10.12, $P = 0.982$). As expected while the time resolution is better and frequency resolution is poorer for shorter windows, the time resolution is poorer and the frequency resolution is better for longer windows. Correspondingly, the mean HWMT was the best for the 16 point window size (9.21 ms, SD = 9.76) and the mean HWMF was the best for 512 point window size (225.72, SD = 211). This is illustrated in Fig. 2. Here, the signal has two humps and a complex frequency structure. It is apparent that the variations in time are well preserved for short window (Fig. 2b). In contrast, the frequency contents of the signal are well preserved for long window (Fig. 2g). A progressive ambiguity in separating two humps with increasing effective window size is clearly illustrated in the plots of normalized instantaneous envelopes (Fig. 2). In contrast, the dominant frequency contents of the signal become more distinctive in the plots of the

normalized spectral energy distributions for the respective effective window sizes (Fig. 2). The mean EBR is lower for shorter windows. However, it increases as a function of window size up to a certain length (128 point), but surprisingly, decreases again with the longer window sizes. As seen in Tables 1B and 2B, the difference between the EBR values for 16 point and 512 point windows was insignificant ($P = 0.509$).

3.3. Effect of window overlap ratio

The mean EBR value increased with increasing overlap ratio as shown in Table 1C. The embolic signal localization also improved as the overlap ratio increased. The mean HWMT appears to increase with increasing overlap ratio. Although overlapping introduces a spread in time and causes an over estimation of the effective embolic signal duration, this does not mean that the time resolution decreases with increasing overlap ratio. The actual time resolution of the WFT is directly determined by the effective window size. In the case of the 0% overlap ratio, the time-frequency

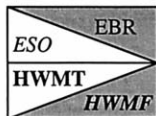
Table 2

Significance values from multiple comparison results for (A) window type, (B) window size and (C) overlap ratio^a

A	Boxcar	-	0.000	0.002	0.000	0.116	0.344
	Bartlett	<i>0.000</i>	-	0.114	0.728	0.004	0.001
	Hanning	<i>0.000</i>	<i>0.000</i>	-	0.037	0.001	0.000
	Hamming	<i>0.000</i>	<i>0.000</i>	<i>0.000</i>	-	0.002	0.001
	Blackman	<i>0.000</i>	<i>0.000</i>	<i>0.000</i>	<i>0.000</i>	-	0.000
	Gaussian	<i>0.000</i>	<i>0.000</i>	<i>0.000</i>	<i>0.000</i>	<i>0.000</i>	-
	Time_eso	<i>0.000</i>	<i>0.001</i>	<i>0.002</i>	<i>0.002</i>	<i>0.056</i>	<i>0.153</i>
	Window type	Boxcar	Bartlett	Hanning	Hamming	Blackman	Gaussian
	Gaussian	0.000	0.000	0.000	0.000	0.007	-
	Blackman	0.000	0.000	0.000	0.000	-	<i>0.021</i>
Hamming	0.000	0.026	0.000	-	<i>0.001</i>	<i>0.000</i>	
Hanning	0.000	0.727	-	<i>0.028</i>	<i>0.032</i>	<i>0.001</i>	
Bartlett	0.000	-	<i>0.054</i>	<i>0.472</i>	<i>0.002</i>	<i>0.000</i>	
Boxcar	-	<i>0.372</i>	<i>0.090</i>	<i>0.427</i>	<i>0.003</i>	<i>0.000</i>	

B	16	-	0.000	0.000	0.000	0.000	0.509
	32	<i>0.473</i>	-	0.000	0.000	0.525	0.003
	64	<i>0.000</i>	<i>0.000</i>	-	0.538	0.001	0.000
	128	<i>0.000</i>	<i>0.000</i>	<i>0.000</i>	-	0.000	0.000
	256	<i>0.000</i>	<i>0.000</i>	<i>0.000</i>	<i>0.000</i>	-	0.000
	512	<i>0.000</i>	<i>0.000</i>	<i>0.000</i>	<i>0.000</i>	<i>0.000</i>	-
	Time_eso	<i>0.982</i>	<i>0.692</i>	<i>0.002</i>	<i>0.000</i>	<i>0.000</i>	<i>0.000</i>
	Window size	16	32	64	128	256	512
	512	0.000	0.000	0.000	0.000	0.000	-
	256	0.000	0.000	0.000	0.000	-	<i>0.598</i>
	128	0.000	0.000	0.000	-	<i>0.000</i>	<i>0.001</i>
	64	0.000	0.000	-	<i>0.000</i>	<i>0.000</i>	<i>0.000</i>
	32	0.031	-	<i>0.000</i>	<i>0.000</i>	<i>0.000</i>	<i>0.000</i>
	16	-	<i>0.000</i>	<i>0.000</i>	<i>0.000</i>	<i>0.000</i>	<i>0.000</i>

C	0%	-	0.001	0.000	0.000	0.000
	25%	<i>0.325</i>	-	0.002	0.000	0.000
	50%	<i>0.953</i>	<i>0.466</i>	-	0.000	0.000
	75%	<i>0.016</i>	<i>0.204</i>	<i>0.188</i>	-	0.000
	98.4%	<i>0.015</i>	<i>0.162</i>	<i>0.162</i>	<i>0.839</i>	-
	Time_eso	<i>0.000</i>	<i>0.000</i>	<i>0.013</i>	<i>0.001</i>	<i>0.002</i>
	Overlap ratio	0%	25%	50%	75%	98.4%
	98.4%	0.000	0.000	0.000	0.000	-
	75%	0.025	0.017	0.111	-	<i>0.322</i>
	50%	0.209	0.155	-	<i>0.269</i>	<i>0.193</i>
	25%	0.880	-	<i>0.166</i>	<i>0.062</i>	<i>0.048</i>
	0%	-	<i>0.492</i>	<i>0.212</i>	<i>0.136</i>	<i>0.122</i>



Key: notation of parameters given in the Table for (A) window type (B) window size and (C) overlap ratio

^a A *P* value of <0.001 was considered as significant. For each parameter, results in shaded normal font in right upper panel represents EBR, results in italic in upper left panel represents ESO, results in bold in lower left panel represents HWMT and results in shaded bold and italic font in lower right panel represents values for HWMF. Notation of parameters given in the Table for (A) window type (B) window size and (C) overlap ratio.

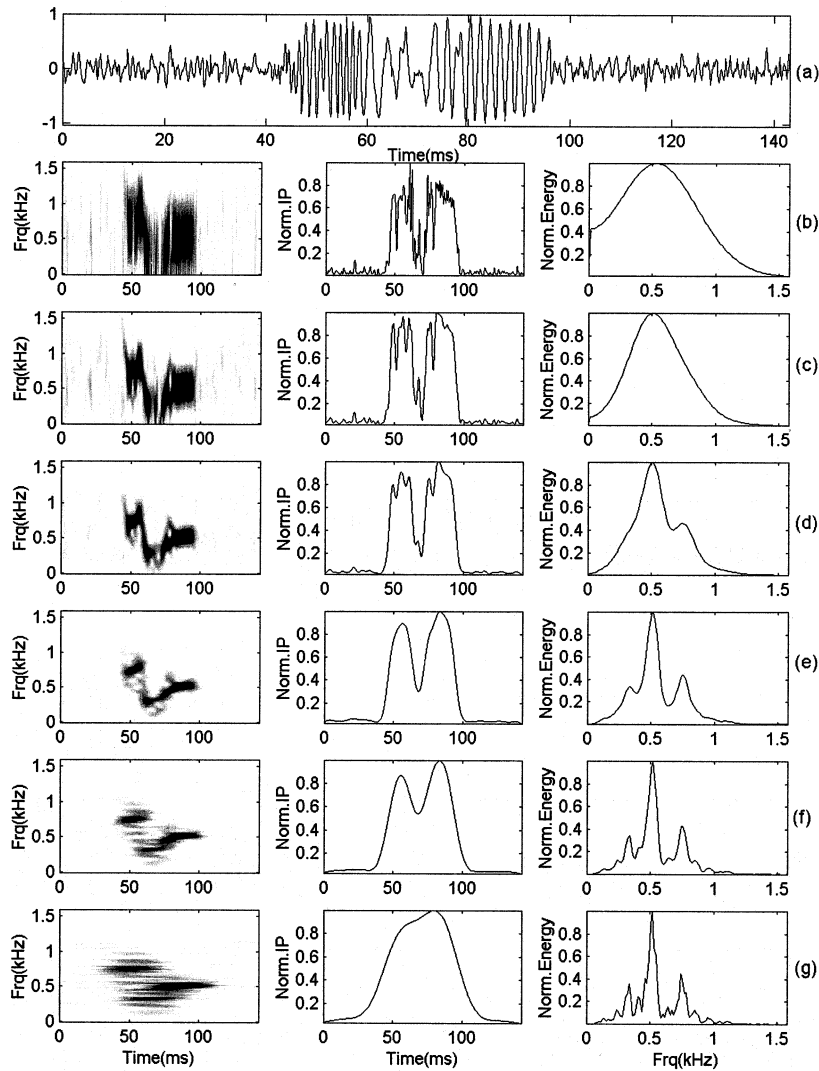


Fig. 2. (a) An embolic signal (only forward flow component) having a complex amplitude and frequency structure, related time-frequency distribution, normalized instantaneous power and normalized energy spectrum for (b) 16 point, (c) 32 point, (d) 64 point, (e) 128 point, (f) 256 point, and (g) 512 point effective window (Hanning) sizes.

representation of the signals is said to be critically sampled. If the embolic signal appears at the correct place within the analysis frame when a non-rectangular window function used, then it will be detected with no ambiguity but with less time resolution. There is a direct relation between the window size (or signal duration relative to the analysis window size) and required overlap ratio for reliable detection. In Fig. 3, change in the EBR, the ESO and the HWMT as a function of

overlap ratio with 32 point (Fig. 3b), 64 point (Fig. 3c), 128 point (Fig. 3d) and 256 point (Fig. 3e) window sizes (Hanning window) for four simulated signals having different durations (Fig. 3a) are presented. Because the windowing function suppresses signals near the edges of the frame there is a possibility that a short embolic signal occurring at the edges of the processing frame may be suppressed and missed as illustrated in Figs. 3 and 4. Fig. 4 illustrates change in the

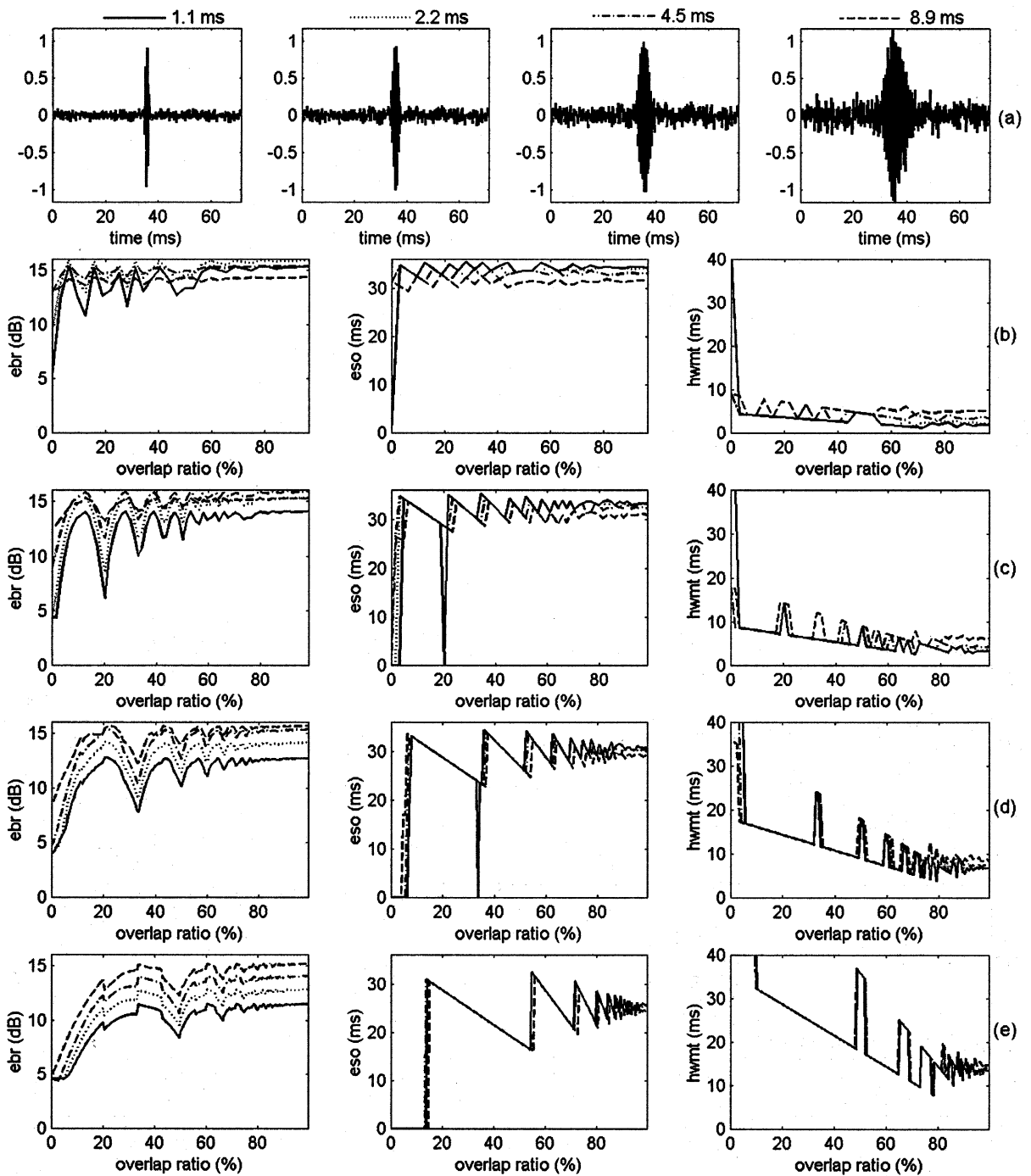


Fig. 3. (a) Simulated embolic signals and corresponding plots showing the change in the EBR, ESO and HWMT as a function of overlap ratio for (b) 32 point, (c) 64 point, (d) 128 point, and (e) 256 point window (Hanning) sizes. The shortest duration (1.1 ms) signal occurring at the edges of the frame is suppressed by the windowing function leading to the dropouts at 20% overlap in (c) and 35% overlap in (d).

EBR, the ESO and the HWMT as a function of overlap ratio with different window types for the simulated short duration (1.1 ms) embolic signal (the FFT size were fixed to 128 point). Again the signal happens to be exactly at the edges of the consecutive frames, so that it is suppressed by windowing function leading to bizarre behavior of the EBR, ESO and HWMT up to 10% and around 33% overlap. It should also be noted that the plots for boxcar window show a stable behavior for almost all overlap ratios. This is because the boxcar window simply does not suppress the signal towards each end of the processing frame. These results demonstrate that it is necessary to employ an overlap of at least approximately 55% for a 32 point window, 65% for a 64 point window, 80% for a 128 point window and 90% for a 256 point window in order to detect very short embolic signals reliably.

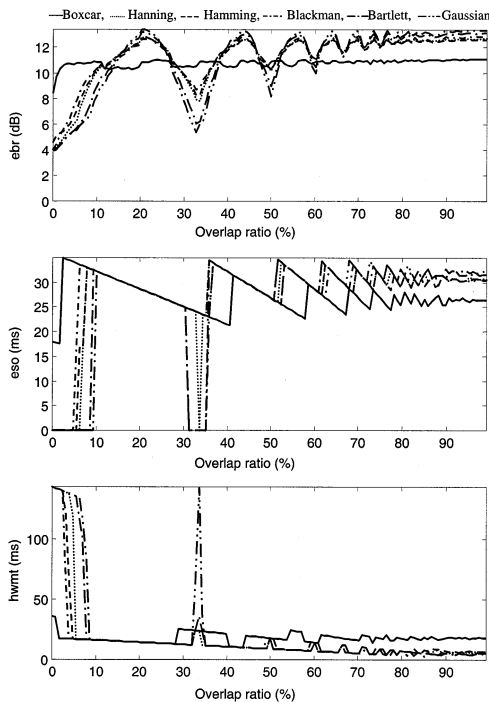


Fig. 4. The change in the EBR, ESO and HWMT as a function of overlap ratio for a simulated short duration (1.1 ms) embolic signal for different window types (FFT size = 128 point). The signal occurring at the edges of the frame is suppressed by the windowing function leading to bizarre behavior of the EBR, ESO and HWMT up to 10% and around 33% overlap.

4. Discussion and conclusion

The results demonstrate the importance of optimizing processing parameters for the detection and analysis of small and very short duration embolic signals, which are those most difficult to detect. Since it has a direct effect on the time-frequency limitation of the FFT, the analysis window size is the most influential parameter. However, the FFT size may be much longer than the effective analysis window as described above. This produces an interpolated FFT result, which is easy to interpret for short windows. This process is virtually equivalent to windowing a signal with a window having the length of W , then zero padding to the FFT length N and taking the FFT.

Relative to the duration of non-stationary variations in a signal, a short window captures the local properties while long window captures the global properties of the signal. According to the results obtained quantitatively and qualitatively, a short window introduces broadening in frequency (spectral broadening) while a long window introduces broadening in time. These two extreme cases appear to cause a decrease in the EBR ratio by possibly increasing the background level in either the frequency (short window) or time space (long window). In contrast, medium-sized windows (64 point (8.9 ms) or 128 point (17.9 ms)) are optimal for embolic signal detection as they reflect the time-frequency behavior of an embolic signal most clearly (Fig. 1d,e). For embolic signals, improvement in frequency resolution (HWMF) was insignificant for window lengths longer than 128 point ($P = 0.598$ for 256 and 512 point windows) as evidenced in Table 2B. Conversely improvement in time resolution (HWMT) was insignificant for window lengths less than 64 point ($P = 0.031$ for 32 and 16 point windows).

In FFT processing, a windowing function is applied mainly to reduce the signal distortion introduced by data segmentation. However this affects the manner in which energy is localized in each time-frequency cell of a time-frequency distribution. The extent to which both spectral resolution and spectral leakage are reduced depends on the window type. The resolution of a window is primarily influenced by the width of the main-

lobe of the window's Fourier transform and spectral leakage by the amplitudes of the sidelobes. A rectangular (boxcar) window has maximum frequency resolution but is worst for spectral leakage (sidelobe distortion). All other window types sacrifice frequency resolution in order to obtain a reduced spectral leakage. The Gaussian window gives the best temporal resolution because the FFT of Gaussian window is still Gaussian having a minimum spread and the Gaussian windows have the minimum time-bandwidth product determined by uncertainty principle (Mallat, 1998).

Although the effect is small, the window type also has an effect on the time-frequency localization and the EBR. Because the windowing function suppresses signals near the edges of the frame there is a possibility that a short embolic signal occurring at the edges of the processing frame may be suppressed and missed as illustrated in Figs. 3 and 4. In practice an adequate overlapping process may overcome this. The required overlap ratio for an embolic signal is a function of its duration and that of the analysis window. This ratio should be determined empirically. In order to cover most embolic signals, 55–95% overlap ratios depending on the window size should be employed as illustrated in Fig. 3. However the overlapping process will generate a data set which is redundant. Although the redundant data is useful for visual presentation, it is best to have as small as possible a feature set for detection and classification, especially in the context of real-time implementations. The EBR increases with increased overlap ratio in general, an effect which should be attributed to the use of data samples more than once producing an averaging effect on the time-frequency representation of the signal. This will obviously decrease the background noise level. Increasing overlap ratio means decreasing the length of actual processing window (less novel samples), i.e. increased temporal resolution. Although this produces a smoother spectrum, it introduces a spread in time causing an over-estimation of the duration of actual embolic signal. However this is not independent of the effective window size, which is the main parameter to be

considered. It also imposes a computational burden on a system in real-time applications.

From the quantitative and the qualitative results of this study, we conclude that a medium size (64 point (8.9 ms) or 128 point (17.9 ms)) FFT with a Hamming, Hanning or Bartlett window is appropriate for detection and analysis of the most embolic signals using the FFT, and the degree of overlap ratio should be as in Fig. 4, usually in the range of 55–97% to avoid any degradation of actual power level of an embolic signal.

Acknowledgements

This work was supported by a British Heart Foundation project grant (PG99064).

References

- Aaslid R, Markwalder T, Nornes H. Noninvasive transcranial Doppler ultrasound recording of flow-velocity in basal cerebral arteries. *J Neurosurg* 1982;57:769–74.
- Aydin N, Padayachee S, Markus HS. The use of the wavelet transform to describe embolic signals. *Ultrasound Med Biol* 1999;25:953–8.
- Boashash B. Estimating and interpreting the instantaneous frequency of a signal: a tutorial review – Part 2: algorithms and applications. *Proc IEEE* 1992;80:539–68.
- Cohen L. Time frequency distributions – a review. *Proc IEEE* 1989;77:941–81.
- Fan L, Evans DH. A real-time and fine resolution analyser used to estimate the instantaneous energy distribution of Doppler signals. *Ultrasound Med Biol* 1994;20:445–54.
- Harris FJ. On the use of windows for harmonic analysis with discrete Fourier transform. *Proc IEEE* 1978;66:51–83.
- Kay SM. *Modern Spectral Estimation*. Englewood Cliffs, NJ: Prentice Hall, 1988.
- Mallat S. *Wavelet Tour of Signal Processing*. San Diego, CA: Academic Press, 1998:30–5.
- Markus HS. Importance of time-window overlap in the detection and analysis of embolic signals. *Stroke* 1995;26:2044–7.
- Markus HS, Tegeler C. Experimental aspects of high-intensity transient signals in detection of emboli. *J Clin Ultrasound* 1995;23:81–7.
- Markus HS, Harrison MJ. Microembolic signal detection using ultrasound. *Stroke* 1995;26:1517–9.
- Markus HS, Ackerstaff R, Babikian V, et al. Inter-centre agreement in reading Doppler embolic signals: a multicentre international study. *Stroke* 1997;28:1307–10.

Ringelstein EB, Droste DW, Babikian VL, et al. International Consensus Group on Microembolus Detection. Consensus on microembolus detection by TCD. *Stroke* 1998;29:725–9.

Spencer MP, Thomas GI, Nicholls SC, Sauvage LR. Detection of middle cerebral emboli during carotid endarterec-

tomy using transcranial Doppler ultrasonography. *Stroke* 1990;21:415–23.

Williams WJ, Sang T, O'Neill JC, Zalubas EJ. Wavelet windowed time-frequency distribution decompositions. *Proceedings of the Society of Photo-Optical Instrumentation Engineers (SPIE)* 1997;3162:149–60.